STEM CELLS AND DEVELOPMENT
Volume 29, Number 18, 2020

DOI: 10.1089/scd.2020.0057

Microbiota-Derived Short-Chain Fatty Acids Promote BMP Signaling by Inhibiting Histone Deacetylation and Contribute to Dentinogenic Differentiation in Murine Incisor Regeneration

Yi Ren,[1] Shenping Su,[1] Xingyu Liu,[1] Yi Zhang,[2] Yuming Zhao,[1] and E. Xiao[2,3]

Microbiota and their metabolites short-chain fatty acids (SCFAs) have important roles in regulating tissue regeneration and mesenchymal stem cell (MSC) differentiation. In this study, we explored the potential effects of SCFAs on murine incisor regeneration and dental MSCs. We observed that SCFA deficiency induced by depletion of microbiota through antibiotic treatment led to lower renewal rate and delayed dentinogenesis in mice incisors. Supplementation with SCFAs in drinking water during antibiotic treatment can rescue the renewal rate and dentinogenesis effectively. In vitro, stimulation with SCFAs could promote differentiation of dental MSCs to odontoblasts. We further found that SCFAs could contribute to dentinogenic differentiation of dental MSCs by increasing bone morphogenetic protein (BMP) signal activation. SCFAs could inhibit deacetylation and increase BMP7 transcription of dental MSCs, which promoted BMP signaling. Our results suggested that SCFAs were required for incisor regeneration as well as differentiation of dental MSCs. Microbiota and their metabolites should be concerned as important factors in the tissue renewal and regeneration.

Keywords: dental mesenchymal stem cell, SCFA, regeneration, BMP signaling, histone deacetylation

Introduction

Mesenchymal stem cell (MSC)-mediated tissue regeneration has been postulated to be a promising therapeutic strategy. MSCs play roles in tissue regeneration and renewal mainly based on their self-renewal capacity and potential for multipotent differentiation. Understanding the biology and regulation networks of MSCs both in vivo and in vitro is crucial for their applications in tissue or organ regeneration.

A large number of bacteria, archaea, viruses, and eukaryotes inhabit the gut of mammals. The microorganism coexisting with their hosts are referred as the microbiota [1]. Microbiota are needed to maintain MSC function and tissue homeostasis in multiple organs. For example, microbiota have shown to be required for the turnover and regeneration of bone as well as the osteogenic differentiation of bone marrow mesenchymal stem cells (BMMSCs) [2–5]. Two main signals from microbiota to distant organs and relevant stem cell niches have been proposed to explain their regulatory effects [6,7].

The first signals are structural components such as lipopolysaccharide (LPS), which are recognized by pattern-recognition receptors, such as Toll-like receptors, NOD-like receptors, and RIG-1-like receptors [8,9]. Structural components can stimulate the immune system to make responses. The second signals are short-chain fatty acids (SCFAs), which are the major fermentation products generated from degradation of dietary fiber by gut microbiota. SCFAs are one to six carbon chain fatty acids, including formate, acetate, propionate, butyrate, isobutyrate, valerate, and isovalerate. In mice, acetate (C2), propionate (C3), and butyrate (C4) are the major types of SCFAs. The concentrations of other types are very low [10–12]. The regulatory effects of SCFAs on host metabolic processes and immune status have been reported a lot [13].

Recent studies have revealed that SCFAs also have an impact on cell fate, including regulation of stem cell function, such as proliferation capacity and differentiation potential [2,14–16]. It has been suggested that SCFAs regulate cell fate mainly by inhibiting activity on histone deacetylases (HDACs). The latter are a class of enzymes that remove acetyl groups from an ε-N-acetyl lysine amino acid on histones, allowing the histones to ''wrap'' the DNA more tightly. These DNA become less accessible to gene transcription factors and are less transcribed as a result. SCFAs can inhibit HDAC activity and increase acetylation of histone H3 as well as transcription of some genes [17].

Departments of [1]Pediatric Dentistry, and [2]Oral and Maxillofacial Surgery, Peking University School and Hospital of Stomatology, Beijing, China.
[3]Department of Stomatology, First People's Hospital of Jinzhong, Jinzhong, China.

Dental MSCs have been regarded as potential stem cells for tissue regeneration application. In vivo, dental MSCs have important roles in the tissue repair and regeneration of teeth [18]. Distinct from other MSCs, dental MSCs have an excellent animal model for in vivo researches. In non-growing teeth such as human teeth and mouse molars, dental MSCs are quiescent and activated only after stimulations to repair damaged dentine.

Mouse incisors, however, maintain continuous growth to replace tissues lost from the tips by grinding. A clearly identifiable population of active dental MSCs, also termed dental pulp stem cells (DPSCs), can be visualized in the proximal core of the incisors between the epithelial cervical loops. These MSCs give rise to a spatially distinct transit-amplifying cell (TAC) population of rapidly proliferating cells that differentiate into odontoblasts and fibroblastic pulp cells. In adulthood, tissue regeneration in mouse incisor is achieved by MSCs/TACs transition, the subsequent TAC-preodontoblast/odontoblast transition and odontoblast differentiation [19–21]. The mouse incisors thus provided not only a highly accessible stem cells source but also a tractable model system to study the function and properties of MSCs in vivo.

Recent studies use cell lineage to analyze the niche environment, where these MSCs reside and how they are regulated in vivo. Those studies have improved our understanding of the in vivo regulatory network involved in regulating MSC fate to support tissue regeneration [22,23]. However, the regulation of incisor regeneration and dental MSCs is incompletely understood. Recently, it has been reported that normal microbiota are needed to maintain gingival MSC regeneration and gingival wound healing, which suggests a link between oral MSCs and microbiota [7]. Furthermore, researchers have found that just like BMMSCs, dental MSCs can also be regulated by SCFAs on differentiation in vitro. Inspired by such findings, we proposed that dental MSCs may also be affected by microbiota and SCFAs.

We hypothesized that microbiota and their metabolite SCFAs affected incisor regeneration and the function of dental MSCs. Broad-spectrum antibiotic treatment has been commonly used in studies exploring the association between normal microbiota and the function of multiple organs [5,7]. Consequently, we intended to deplete microbiota and downgrade SCFA levels through broad-spectrum antibiotic treatment to explore the possible links between microbiota/SCFAs and dental MSCs.

Materials and Methods

Ethics approval of the study protocol

The protocol of animal experiments was approved by the Ethics Committee of the Peking University Health Science Center (no. LA2018184) in Beijing, China.

Mice and antibiotic treatment

Four-week-old C57BL/6 female mice were divided randomly into four groups. Mice in the antibiotic-treated (ABX) group were given antibiotic water containing ampicillin (1 g/L), neomycin (1 g/L), metronidazole (1 g/L), and vancomycin (0.5 g/L). Mice in the specific pathogen-free (SPF) group were fed with sterile distilled water as the control. After 6 days of antibiotic treatment, mice in the Co-house group were cohabited with mice in the SPF group and fed the same water for 3 days. Mice in the SCFA group were given antibiotic water containing SCFAs (150 mM of acetate, propionate, and butyrate, Sigma-Aldrich, Saint Louis, MO) for 9 days.

Incisor clipping experiments

After 9 days of treatment with different types of water, mice were anesthetized with sodium pentobarbital (i.p.). Clipping was undertaken by removing the upper 1.5–2 mm of the erupted part of the lower incisor on one side using a diamond cylinder bur with a high-speed handpiece. To monitor the growth-rate changes of incisors, photographs of the clipped incisors were taken by the same device every 24 h for 3 days. The images were analyzed by ImageJ (National Institutes of Health, Bethesda, MD).

Incorporation of 5-Bromo-2-DeoxyUridine

For labeling of slow-cycling cells, 5-Bromo-2-DeoxyUridine (BrdU) (Sigma-Aldrich) was given daily (40 μg/g bodyweight, i.p.) from P5 to P9 and traced for 4 weeks. Mice were divided into different groups 19 days after the last BrdU injection and treated with different types of water. The clipping was done after treatment with different types of water, the time 4 weeks after BrdU injection. For TACs labeling, BrdU (40 μg/g bodyweight, i.p.) was injected into mice 2 h before sacrifice.

Isolation, culture, and mineralization of mouse DPSCs

Mouse DPSCs were isolated from the lower incisors of mice, as described previously [24]. Cells were cultured in α-modified minimum essential medium (Gibco, Grand Island, NY) containing 20% fetal bovine serum (Gibco), ascorbic acid (10 mM; Gibco), and glutamate (2 mM; Gibco) at 37°C in an atmosphere of 5% carbon dioxide. Mineralization medium was supplemented with 10 nM dexamethasone (Sigma-Aldrich) and 10 mM β-glycerophosphate (Sigma-Aldrich).

Cell proliferation assay

Primary DPSCs were seeded at 4,000 cells/100 μL per well in 96-well plates. The cell number was assessed on days 2, 4, 6, 8, and 10 by the Cell Counting Kit-8 (CCK-8; Dojindo Laboratories, Kumamoto, Japan) according to the manufacturer's instructions. Briefly, 10 μL of CCK-8 solution was added to each well and incubated for 2 h. Absorbance at 450 nm was measured. Results were representative of three individual experiments.

Colony-forming assay

Primary DPSCs were counted and seeded at 500 cells in 35-mm dishes. After 10 days of primary culture, cells were washed thrice with 1 × phosphate-buffered saline (PBS) and fixed with 1 mL of 4% formalin for 30 min at room temperature. Formalin was removed and cells were washed with PBS. Then, 1 mL of 0.5% Crystal Violet (Zhongshan Biosciences, Beijing, China) was added to dishes and incubated for 10–15 min at room temperature. PBS was used to gently wash excess Crystal Violet.

Alizarin Red S staining

Cells were cultured in six-well plates with mineralization medium for 7 days before staining with Alizarin Red S. For staining, cells were washed thrice with 1 × PBS and fixed with 1 mL of 4% formalin at room temperature. Thirty minutes later, formalin was removed and cells were washed thrice with distilled water. Then, 1 mL of freshly made 2% Alizarin Red S solution (pH 4.2; Sigma-Aldrich) was added into plates. After a 30-minute incubation at room temperature, the plates were gently washed with distilled water to remove excess Alizarin Red S. The staining area was analyzed with ImageJ. The group cultured with mineralization medium was regarded as the control. Groups cultured with mineralization medium supplemented with sodium acetate (C2) or sodium butyrate (C4) were compared with the control.

SCFA measurement

The gas chromatography–mass spectrometry system was fitted with a capillary column Agilent HP-INNOWAX (30 m × 0.25 mm i.d., film thickness = 0.25 μm; Agilent Technologies, Santa Clara, CA). Helium was used as the carrier gas at 1 mL/min. Injection was made in split mode at 10:1 with an injection volume of 1 μL and an injector temperature of 250°C. The temperature of the ion source, interface, and quadrupole were 230°C, 250°C, and 250°C, respectively. The column temperature was 90°C initially. Then it was increased to 120°C at 10°C/min, to 150°C at 5°C/min, and finally to 250°C at 25°C/min and maintained at this temperature for 2 min (total run time of 15 min). The detector was operated in electron impact ionization mode using full scan and selected ion monitoring mode.

Quantitative reverse transcription–PCR

Total RNA was extracted from cells by TRIzol® Reagent (Life Technologies, Carlsbad, CA), and reverse transcription was carried out with moloney murine leukemia virus (M-MLV) reverse transcriptase (Promega, Fitchburg, WI) according to the manufacturer's instructions. Quantification of messenger RNA (mRNA) expression was achieved using FastStartTM Universasl SYBR Green Master (ROX) Reagent (Roche, Basel, Switzerland) on an ABI StepOnePlusTM Real-Time PCR system. The mRNA expression of genes of interest were normalized to that of β-actin, and the results were represented as fold change using the $2^{C\tau\Delta\Delta}$ method. Primer sequences are shown in Supplementary Figure S1a.

Histology and fluorescence in situ hybridization

Dissected mandibles were fixed in 4% paraformaldehyde overnight at 4°C, and then decalcified in 10% diethylpyrocarbonate-treated (DEPC-treated) ethylenediaminetetraacetic acid (EDTA) (pH 7.4) for 2 weeks. Samples were dehydrated through serial concentrations of ethanol for paraffin embedding. Hematoxylin and eosin (H&E) staining was carried out on deparaffinized sections (4 μm) following standard procedures. For the detection of the dentin sialophosphoprotein (*DSPP*), fluorescence in situ hybridization was done using the RNA Labeling Kit (GenePharma, Shanghai, China) according to the manufacturer's instructions.

Immunofluorescence staining

The tissue sections were deparaffinized and rehydrated by xylene and gradient ethyl alcohol. Antigen retrieval was performed in 0.01 M sodium citrate buffer (pH 6.0) for 30 min at 95°C or in EDTA buffer (pH 9.0) for 30 min at 95°C (Psmad1/5/9). Consequently, sections were treated with 3% (w/v) hydrogen peroxide for 20 min, permeabilized with 0.5% Triton X-100 for 10 min, and blocked with 10% blocking buffer at room temperature for 1 h. Sections were then incubated with primary antibodies diluted in Antibody Diluent (Zhongshan Biosciences) overnight at 4°C followed by the appropriate secondary antibodies. 4′ 6-diamidino-2-phenylindole (DAPI) (Zhongshan Biosciences) was used for staining of cell nuclei. Finally, all images were analyzed using an optical microscope (Olympus, Tokyo, Japan).

The following antibodies were used to carry out immunostaining: BrdU (1:300; ab6326; Abcam, Cambridge, UK), Ki67 (1:100; ab15580; Abcam), Gli1 (1:500; NBP1-78259; Novus Biological), dentin matrix protein-1 (DMP-1) (1:300; ab103203; Abcam), phosphorylated Smad1/5/9 (Psmad1/5/9) (1:500; 13820; Cell Signaling Technology, Danvers, MA); and bone morphogenetic protein (BMP)7 (1:1,000; ab56023; Abcam). Alexa Fluor 488 (1:200; ab150081; Abcam) and rhodamine-conjugated goat anti-rat immunoglobulin G (IgG) (Zhongshan Biosciences) were used for signal detection. The Alexa Fluor 488 Tyramide SuperBoostTM Kits (B40922; Invitrogen) were used for Psmad1/5/9 and Gli1.

Western blot

Total protein was extracted from the cells using RIPA Buffer (Beyotime, Jiangsu, China) supplemented with protease inhibitor and phosphatase inhibitor. Protein concentrations were determined using the Bicinchoninic Acid Protein Assay Kit. Then, 60 μg of total protein was separated by electrophoresis in 10% (w/v) sodium dodecyl sulfate–polyacrylamide gel and was then transferred to polyvinylidene fluoride membranes (Bio-Rad Laboratories, Hercules, CA). Membranes were blocked with Tris-buffered saline containing 0.05 % Tween-20 (TBST) containing 5% (w/v) non-fat milk for 1 h at room temperature.

The membranes were blotted with antibodies against alkaline phosphatase (ALP) (1:1,000; ab108337; Abcam), DSPP (1:500; sc-73632; Santa Cruz Biotechnology, Santa Cruz, CA), DMP-1 (1:1,000; ab103203; Abcam), Psmad1/5/9 (1:1,000; 13820; Cell Signaling Technology), Acetyl-Histone H3 (AcH3) (1:1,000; 06-599; EMD Millipore, Burlington, MA), BMP7 (1:1,000; ab56023; Abcam), and glyceraldehyde-3-phosphate dehydrogenase (GAPDH) (Zhongshan Biosciences) diluted in 5% (w/v) bovine serum albumin (BSA)-TBST on a shaker overnight at 4°C. After washing thrice with TBST, membranes were incubated with horseradish peroxidase (HRP)-conjugated secondary antibodies. Protein bands were visualized by enhanced chemiluminescent detection reagent (CW Biotech, Beijing, China) and exposed to X-ray film. Band intensities were quantified using ImageJ. The background was subtracted, and the signal of each target band was normalized to that of the GAPDH band.

Chromatin immunoprecipitation

Chromatin immunoprecipitation (ChIP) assay was done using the EZ-Magna ChIP Kit (EMD Millipore) according to the

manufacturer's instructions. Briefly, cells were crosslinked with 37% formaldehyde, pelleted, and resuspended in nuclear lysis buffer. Sonication was undertaken to shear the chromatin to a manageable size. Centrifugation was carried out to remove insoluble material. Supernatants were collected and incubated with Anti-AcH3 (06-599; EMD Millipore), normal rabbit IgG (12-370; EMD Millipore), and magna beads overnight. The beads were removed and the precipitated chromatin complexes were collected, purified, and decrosslinked for 2 h at 62°C, followed by DNA purification and real-time PCR detection. Primer sequences are shown in Supplementary Figure S1a.

Enzyme-linked immunosorbent assay

Enzyme-linked immunosorbent assay (ELISA) was done using the Mouse BMP7 ELISA Kit (Qisong Biology, Beijing, China) according to the manufacturer's instructions. Cell supernatants were collected by centrifugation after 3-day culture in mineralization medium or mineralization medium supplemented with C2/C4 treatment. Cell supernatants cultured in mineralization medium alone were regarded as the control. Cell supernatants were stored at −20°C. All reagents were allowed to reach room temperature before use. Then, 50 μL of a prepared standard was added to standard wells. Ten μL of samples and 40 μL of dilution buffer were added to test wells. The plate was covered with an adhesive strip and incubation instigated for 2 h at room temperature. The liquid was discarded and each well was washed four times with the washing solution.

The antibody reagent (100 μL) was added to each well. The plate was covered with a strip and allowed to incubate for 1 h at room temperature. The liquid was discarded and each well was washed four times. HRP-conjugate reagent (100 μL) was added to each well. The plate was covered with a strip and incubation for 1 h at 37°C was allowed. The liquid was discarded and each well was washed four times. Chromogenic solution A (50 μL) and solution B (50 μL) were added to each well. The plate was incubated in the dark for 15 min at 37°C. Stop Solution (100 μL) was added to each well. Absorbance at 450 nm was measured with a reader (Infinite F50; Tecan, Switzerland). Excel™ (Microsoft, Redmond, WA) was employed to create a standard curve, and then the results of test samples were calculated.

ImageJ analyses

ImageJ was used to calculate the growth length of clipped incisors. The percentage of positive immunofluorescence signals in immunostained regions, the area of Alizarin Red S staining, and western blots were analyzed by ImageJ.

Statistical analyses

Statistical analyses were undertaken using Prism 6 (GraphPad, San Diego, CA). The Student's *t*-test was used to assess significance between two groups. Data are the mean ± standard deviation. $P < 0.05$ was considered significant.

Results

Antibiotic-induced depletion of microbiota leads to a lower rate of incisor renewal

To explore the possible role microbiota might play in mouse incisor regeneration, mice of ABX group were given a combination of broad-spectrum antibiotics in drinking water for 9 days to deplete the commensal flora before incisor clipping [8]. Consistent with data from other studies [25,26], antibiotic treatment significantly reduced fecal bacterial DNA load and depleted most microbiota in feces ($P < 0.05$, $n = 5$) (Fig. 1b). However, mice co-housed with SPF mice after antibiotic treatment showed no difference in fecal bacterial DNA load compared with SPF mice ($P = 0.36$, $n = 5$).

In normal circumstances, it is difficult to observe and record the daily growth height of mouse incisors directly. To observe and measure the renewal rate of mouse incisors, we removed about 1.5–2 mm of the uppermost erupted part of incisors on one side by clipping. H&E staining showed there were no inflammatory or structural changes after clipping (Supplementary Figure S1b).

The growth height of the clipped incisors was then measured using the same device every 24 h and compared among different groups during the subsequent 3 days. As a result, we observed the growth height of ABX mice to be decreased significantly compared with SPF mice ($P < 0.05$, $n = 5$). Co-housed mice showed no difference compared with SPF mice ($P_{24h} = 0.7343$, $P_{48h} = 0.9838$, $P_{72h} = 0.3599$, $n = 5$) (Fig. 1d–e). The results demonstrated that microbiota affected incisor renewal of mice. Microbiota depletion by antibiotic treatment led to a lower renewal rate of incisors, which could be normalized by microbiota recolonization.

Supplementation with SCFAs during antibiotic treatment can rescue the renewal rate of incisors

To confirm the possible signals from microbiota to distant dental tissues, we first supplied antibiotic-treated mice with LPS during antibiotic treatment. This action did not normalize the growth rate of incisors. We also detected immune cytokines, including interleukin (IL)-1β, IL-10, IL-6, IL-23, tumor necrosis factor-α, and interferon-γ, of dental pulps after antibiotic treatment and the results showed no significant changes among different groups (data not shown). Thus, microbiota might not function by immune signals.

We then found that antibiotic treatment caused a significant reduction in the SCFA levels in serum ($P < 0.05$, $n = 4$) (Fig. 1c). We noted that when SCFA level decreased in ABX group, the incisor renewal rate also decreased, which suggested that the signaling molecules from microbiota might be their most common end metabolite SCFAs.

To clarify it, we added the three main SCFAs (acetate, propionate, and butyrate; 150 mM) to drinking water during antibiotic treatment (SCFA group). The mice supplemented with SCFAs in drinking water showed no difference in SCFA serum levels compared with SPF mice ($P = 0.91$, $n = 4$) (Fig. 1c). Notably the mice in SCFA group also showed no difference in incisor renewal rates compared with SPF mice ($P_{24h} = 0.6002$, $P_{48h} = 0.9840$, $P_{72h} = 0.8407$, $n = 5$). In comparison with ABX mice, the mice in the SCFA group showed increased incisor renewal rates ($P < 0.05$, $n = 5$) (Fig. 1d–e). These results suggested that microbiota affected incisor renewal of mice through SCFAs.

SCFAs promote TAC-preodontoblast/odontoblast transition and dentinogenic differentiation

The mouse incisor is composed of two epithelial and mesenchymal compartments. Both compartments replenish

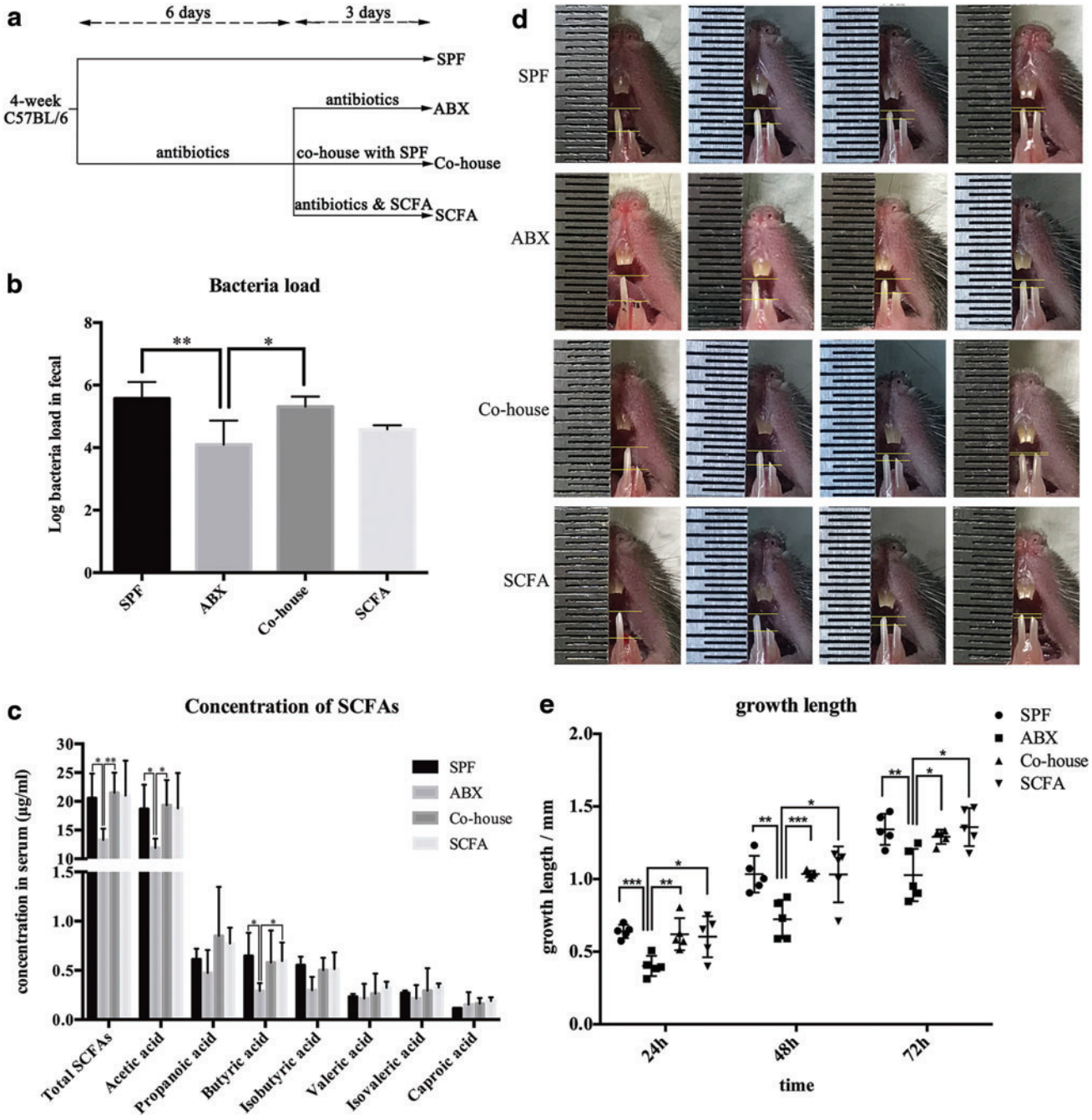

FIG. 1. Antibiotic-induced depletion of microbiota leads to a lower serum SCFA level and incisor renewal rate, which could be rescued effectively by SCFA supplementation. **(a)** Experimental procedure (schematics). **(b)** Total number of bacteria (log 16S rRNA gene copies/g feces) of different groups ($n=5$). **(c)** Concentration of SCFAs in mice serum ($n=4$). **(d, e)** The growth height of clipped incisors in different groups was recorded and measured 24, 48, and 72 h, respectively, after clipping ($n=5$). Data represent Mean ± SEM, $*P<0.05$, $**P<0.01$, $***P<0.001$. ABX, antibiotic-treated; SCFA, short-chain fatty acid; SEM, standard error of the mean; SPF, specific pathogen free. Color images are available online.

all of their cells within 1 month. The continuous renewal of incisors is supported by dental MSCs/DPSCs and epithelial stem cells, both of which divide infrequently and, therefore, retain BrdU labels. We undertook BrdU injection to trace dental stem cells (long-chase label-retaining cells, LRCs) and carried out BrdU immunofluorescence staining (Fig. 2a) [27]. The staining showed that, compared with SPF mice, ABX mice had a smaller population of dental MSCs in both nonclipped incisors and incisors 48 h after clipping ($P<0.05$, $n=5$–6) (Fig. 2b, c, e, f), whereas mice in the Co-house and SCFA group showed no difference compared with SPF mice (Co-house vs. SPF $P_{0h}=0.1817$, $P_{48h}=0.3453$; SCFA vs. SPF $P_{0h}=0.0981$, $P_{48h}=0.3023$, $n=5$–6). Obvious changes in epithelial stem cells were not observed.

To confirm whether BrdU-positive cells were dental MSCs, we carried out double staining of BrdU and Gli1. Gli1 is one of the markers for dental MSCs. The staining showed that the Gli1 expression was detectable in the zone

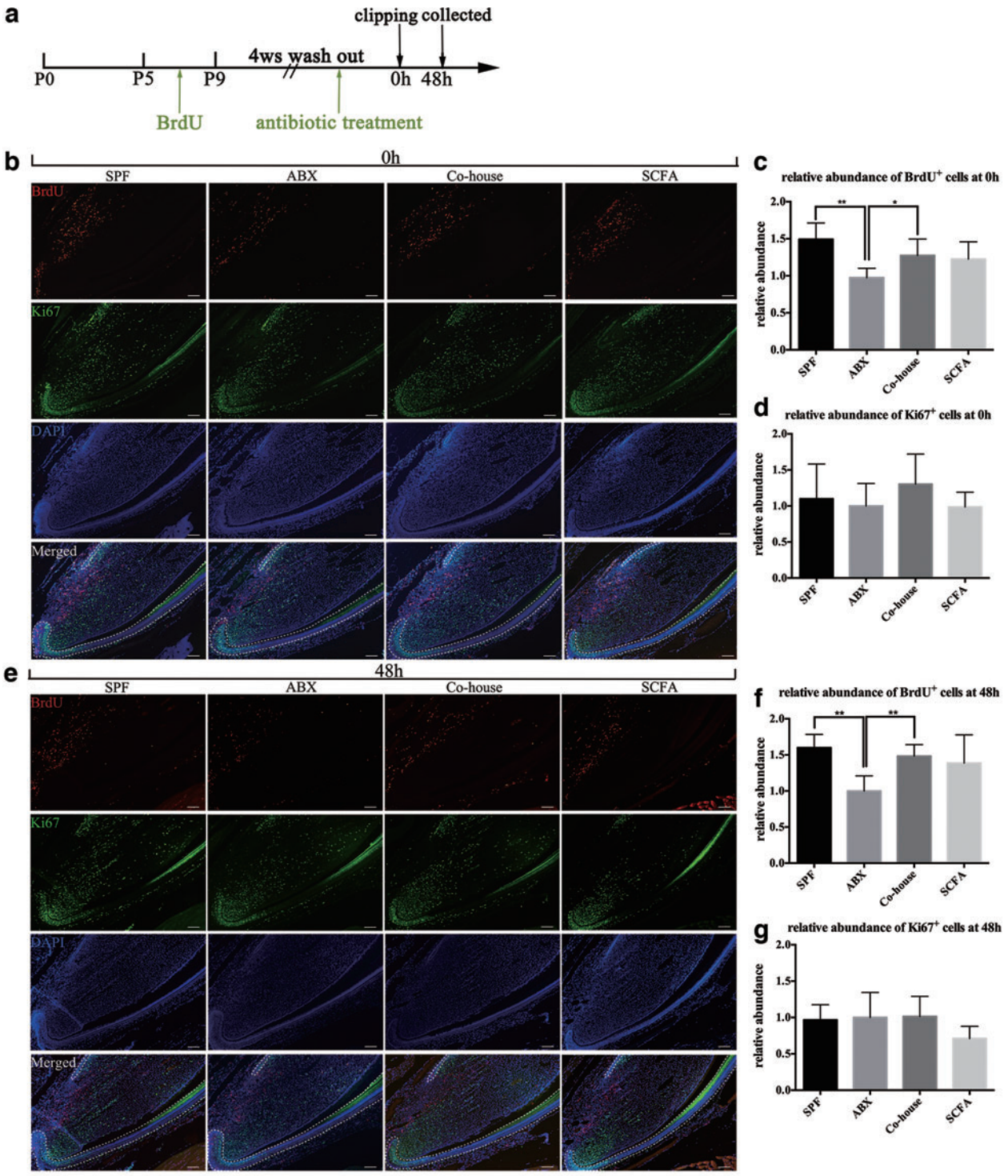

FIG. 2. Antibiotic-induced depletion of microbiota leads to fewer dental MSCs, which can be rescued by SCFA supplementation. **(a)** Experimental design for tracing dental stem cells by BrdU injection. BrdU was administered repeatedly to newborn C57 mice at P5–P9 (*green arrow*), followed by a 4-week injection-free period before clipping. **(b, e)** Immunofluorescent staining of BrdU (*red*) and Ki67 (*green*) in incisors of mice in SPF, ABX, Co-house, and SCFA groups. Samples in **(b)** were collected immediately after clipping, whereas samples in **(e)** were collected 48 h after clipping. *Dotted lines* outlined the cervical loop dental epithelium. Cell nuclei were stained with DAPI (*blue*). Scale bar: 100 μm. **(c, d, f, g)** Quantification of BrdU- and Ki67-positive cells in apical areas of incisors. Quantification was done by ImageJ. Data represent mean ± SEM, $n = 5–6$, $^{*}P < 0.05$, $^{**}P < 0.01$. BrdU, 5-Bromo-2-DeoxyUridine; DAPI, 4′-6-diamidino-2-phenylindole; MSC, mesenchymal stem cell. Color images are available online.

of BrdU-positive cells and a large amount of Gli1-expressing cells colocalizing with BrdU-positive cells (Supplementary Fig. S1c). Then, we carried out Gli1 staining and the results were consistent with BrdU staining (Supplementary Fig. S1d).

During growth, dental MSCs exit from their niche and transit to TACs. The latter can be identified readily based on their active proliferation and give rise to preodontoblasts, terminally differentiated odontoblasts, and dental pulp cells. We performed staining of the proliferation marker Ki67 to ascertain if the decreased MSC population led to less TACs in ABX mice. Surprisingly, the number of Ki67-positive cells (TACs) in ABX mice exhibited no obvious difference compared with SPF mice in both nonclipped incisors and incisors 48 h after clipping ($P_{0h}=0.7072$, $P_{48h}=0.8553$, $n=5$–6) (Fig. 2b, d, e, g). To confirm it, we carried out short-chase BrdU label retaining to trace TACs: the result was consistent with Ki67 staining (Supplementary Fig. S2a). These results demonstrated that the proliferation of dental MSCs was not affected by antibiotic treatment.

In mouse incisor, dentine renewal or regeneration was achieved by MSC-TAC transition and subsequent TAC-pre-odontoblast/odontoblast transition. Since TAC number was not affected by antibiotic treatment, the lower renewal rate of ABX mice may be caused by abnormal TAC-preodontoblast/odontoblast transition. Therefore, we focused on the differentiation process. We examined the TAC-preodontoblast/odontoblast transition by measuring the expression of *DSPP* and DMP-1 in the TAC region. The staining showed that the antibiotic-treated mice had lower expression of these dentin mineralization markers 48 h after clipping compared with SPF mice, whereas mice in SCFA and Co-house group had no difference with SPF mice ($n=4$–6) (Fig. 3a, b).

The results suggested that dentinogenesis was delayed in ABX mice and could be rescued by supplementation with microbiota or SCFAs. SCFAs promoted dentinogenic differentiation in vivo and maintained the dentine regeneration, which may account for the rescued renewal rate in mice of the SCFA group.

We also tested the properties of MSCs in vitro. Mouse DPSCs were isolated from mice incisors in ABX, SPF, and SCFA groups, respectively. The colony-forming assay showed that DPSCs from ABX mice exhibited decreased colony numbers (Fig. 3c). The CCK-8 assay showed no difference in proliferative ability between DPSCs from ABX mice and SPF mice (Fig. 3d). Alizarin Red S staining demonstrated that DPSCs from ABX mice formed fewer mineralized nodules (Fig. 3e, f). These results demonstrated that the self-renewal capacity and differentiation ability of DPSCs in ABX mice were decreased, whereas the proliferative ability was not affected. Such results were consistent with our in vivo results.

To confirm the effect of SCFAs on dentinogenic differentiation, we added different concentrations of SCFAs to stimulate mouse DPSCs and tested the expression of differentiation markers. Considering C2 and C4 exhibited difference between ABX mice and SPF mice (Fig. 1c), we chose C2 and C4 for the in vitro stimulation. Real-time PCR demonstrated an increase in expression of *ALP*, *DSPP*, and *DMP-1* after 5 days of treatment with C2 or C4 of different concentrations (Fig. 4a–c). Western blotting showed an increase in protein expression of ALP, DSPP, and DMP-1 after 7 days of treatment with C2 or C4 of different concentrations (Fig. 4d; Supplementary Fig. S2c). Alizarin Red S staining showed that DPSCs stimulated with C2 or C4 formed more mineralized nodules (Fig. 4e, f).

Taking these results together, we concluded that SCFAs (mainly C2 and C4) promoted dentinogenic differentiation in vivo and in vitro.

SCFAs promote BMP7 expression of dental MSCs by suppressing HDAC activity and contribute to the odontoblast differentiation

Epigenetic regulation has an important role in regulating the potency and lineage commitment of stem cells. Histone acetylation can regulate stem cells by changing gene transcription [28]. As natural inhibitors, SCFAs can inhibit HDAC activity and promote histone acetylation. We measured histone acetylation of DPSCs stimulated with different concentrations of C2 and C4 for 7 days. An increase in acetylation of H3 was observed by western blotting (Fig. 5a; Supplementary Fig. S2c). Hence, C2 and C4 could inhibit HDAC activity and promote histone acetylation in DPSCs.

Studies have suggested that inhibition of HDAC activity affects BMP signaling-induced osteogenic differentiation of MSCs in mice [29]. BMP signaling is crucial for odontoblast differentiation and plays an important part in providing feedback to the MSC populations [30]. We investigated if SCFAs affected dentinogenic differentiation of DPSCs by changing BMP signaling molecules. To test BMP signaling activity, we measured expression of phosphorylated Smad1/5/9 (pSmad1/5/9), a readout of activated BMP signaling. We found that BMP signaling was decreased in ABX mice in the TAC zone between TACs and odontoblasts ($P<0.05$, $n=4$), whereas mice supplemented with SCFAs showed no difference compared with SPF mice ($P=0.83$, $n=4$) (Fig. 5b, c).

In vitro, western blotting demonstrated increased protein expression of pSmad1/5/9 after treatment with C2 or C4 at different concentrations (Fig. 5d; Supplementary Fig. S2c).

Next, we investigated if the increased BMP signaling by SCFAs was related to accelerated transcriptions by histone acetylation in BMP promoter regions. We chose C4 (0.25 μM) for the subsequent ChIP experiment. ChIP analysis was done using antibody against acetylated histone H3 and primers of

FIG. 3. SCFAs promote TAC-preodontoblast/odontoblast transition and odontoblast differentiation. **(a)** Fluorescence in situ hybridization of *DSPP* (*red*) in clipped incisors ($n=4$–6). Boxes are magnified in the fourth *row*. **(b)** Immunofluorescent staining of DMP-1 (*green*) in clipped incisors ($n=4$–6). Boxes are magnified. Samples in **(a)** and **(b)** were collected 48 h after clipping. Cell nuclei were stained with DAPI (*blue*). Scale bar: 50 μm. **(c)** Colony-forming assay of primary DPSCs. **(d)** Cell-proliferation assay (CCK8) of primary DPSCs. **(e)** Alizarin Red S staining. P2 cells were cultured in mineralization medium for 7 days before Alizarin Red S staining. **(f)** Quantification of Alizarin Red S staining. Data were measured by ImageJ and represent two independent experiments. $^*P<0.05$. CCK-8, Cell Counting Kit-8; DSPP, dentin sialophosphoprotein; DMP-1, dentin matrix protein-1; TAC, transit-amplifying cell. Color images are available online.

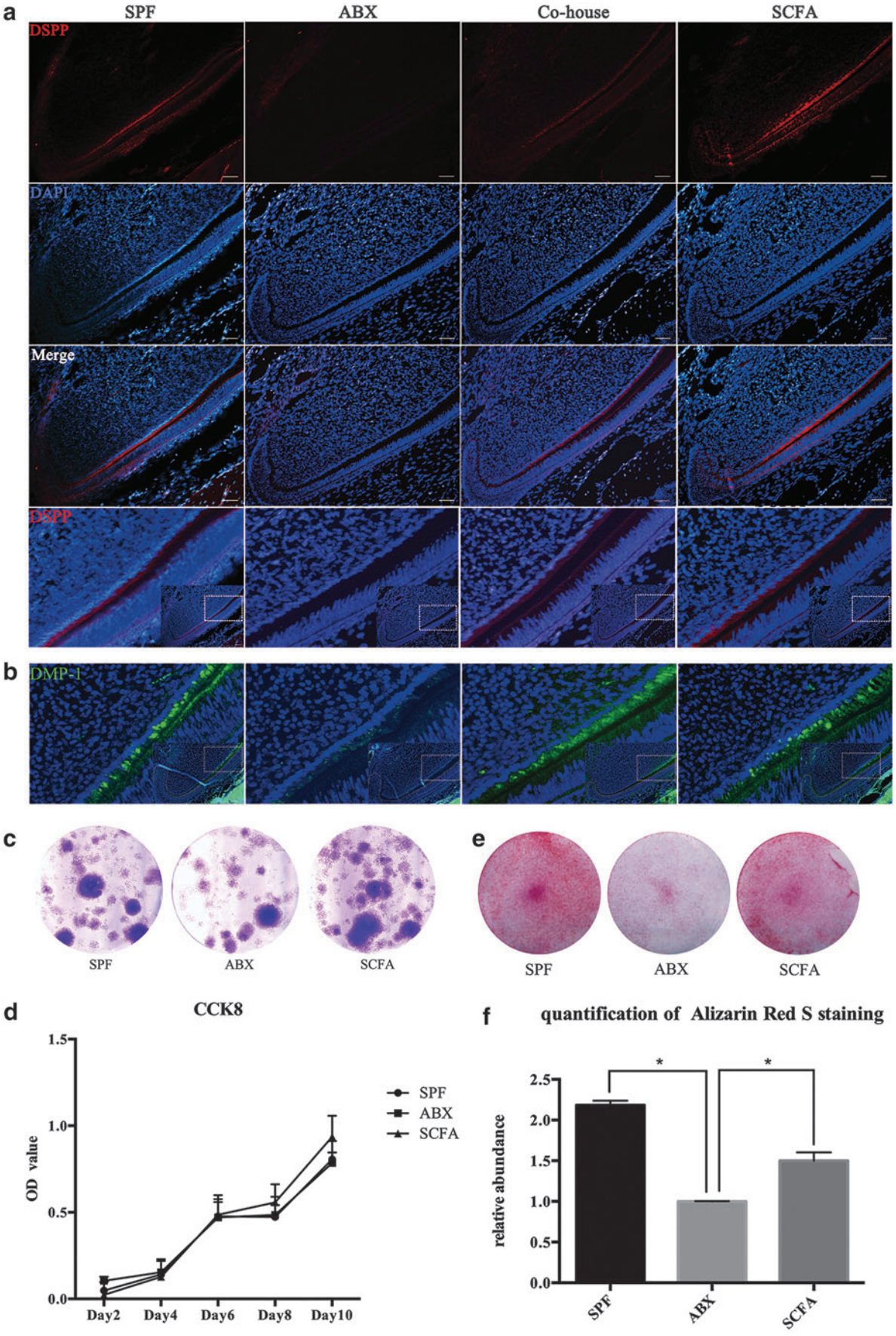

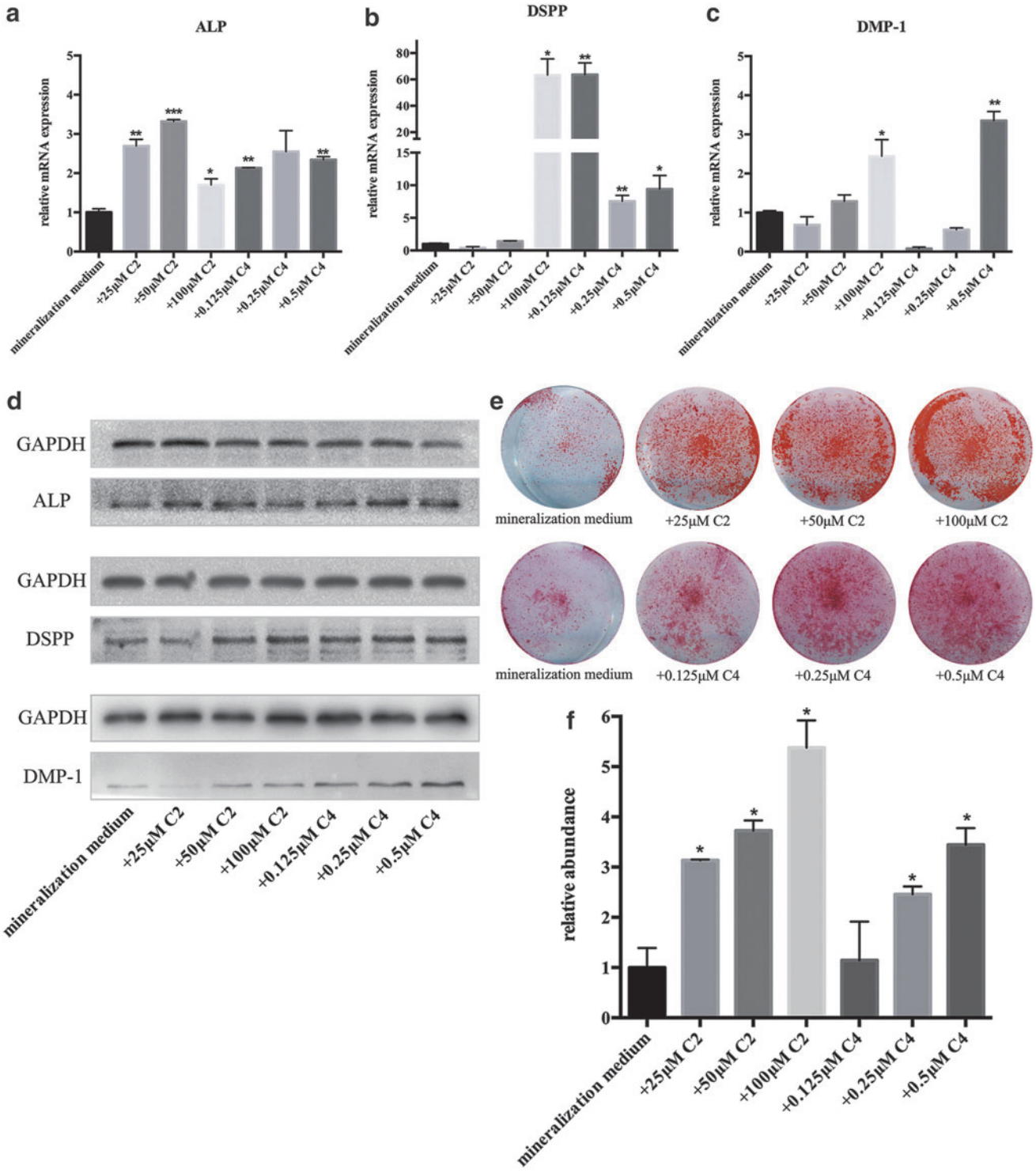

FIG. 4. SCFAs promote the differentiation of dental MSCs to odontoblasts in vitro. **(a–c)** Expression of the odontoblast-differentiation markers *ALP*, *DSPP* and *DMP-1* quantified by real-time PCR. DPSCs were cultured in mineralization medium or mineralization medium supplemented with different concentrations of C2 or C4 for 5 days before real-time PCR. **(d)** Western blots of ALP, DSPP, and DMP-1. **(e, f)** Alizarin Red S staining and quantification. Data were measured by ImageJ and represent two independent experiments. DPSCs were cultured in mineralization medium or mineralization medium supplemented with different concentrations of C2 or C4 for 7 days before western blotting and Alizarin Red S staining. $*P < 0.05$, $**P < 0.01$, $***P < 0.001$. ALP, alkaline phosphatase. Color images are available online.

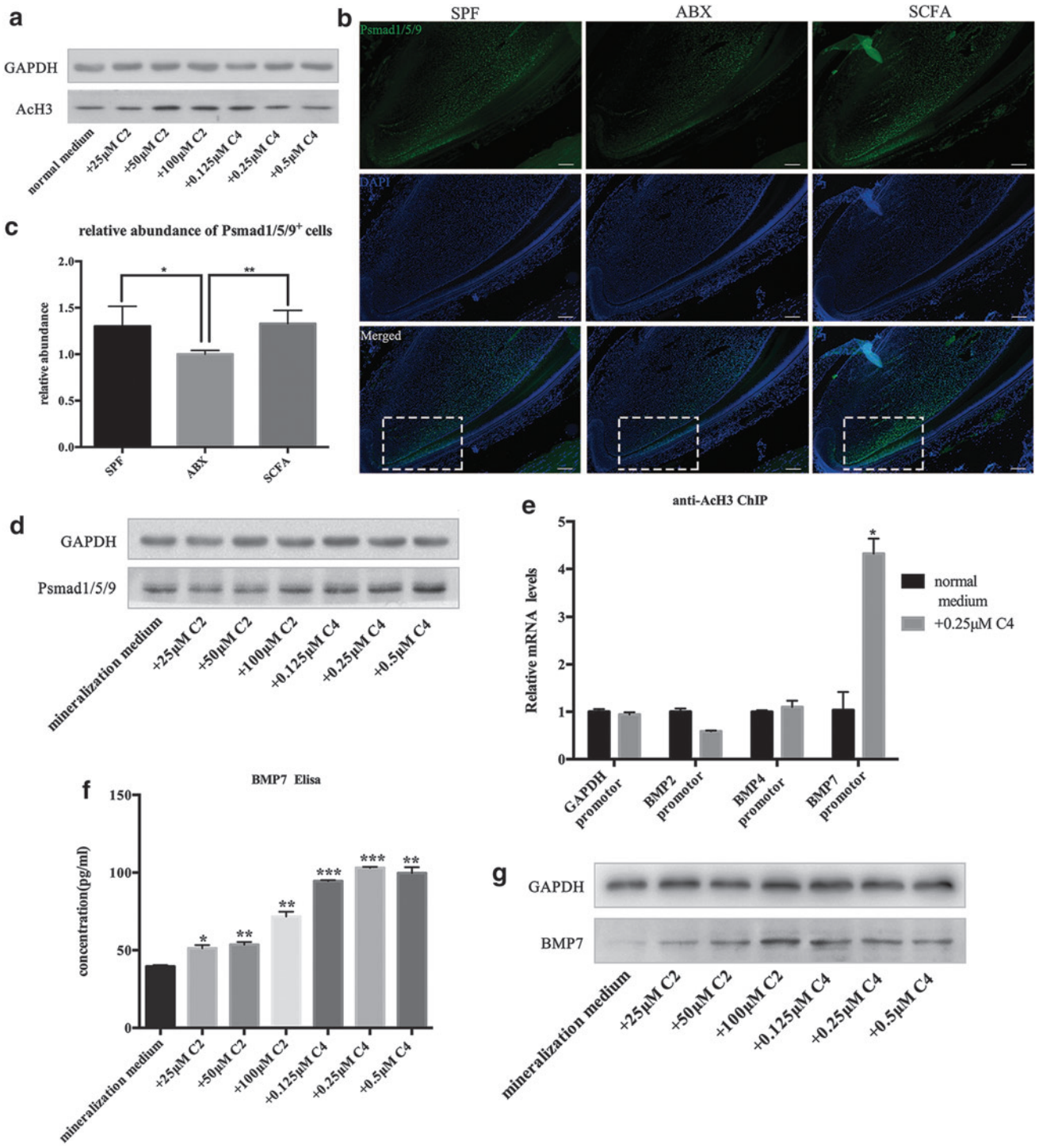

FIG. 5. SCFAs promote BMP7 expression by suppressing HDACs and contribute to the dentinogenic differentiation. **(a)** Measurement of acetylation of histone H3 by western blotting. Mouse DPSCs were cultured in normal medium or normal medium supplemented with different concentrations of C2 or C4 for 7 days before western blotting. **(b)** Immunofluorescent staining of Psmad1/5/9 (*green*) in clipped incisors. Samples were collected 48 h after clipping ($n=4$). Cell nuclei were stained with DAPI (*blue*). Scale bar: 100 μm. **(c)** Quantification of Psmad1/5/9-positive cells in apical areas of incisors ($n=4$). **(d)** Western blots of Psmad1/5/9. **(e)** ChIP assay on BMP promoters. ChIP analysis revealed a significant increase in histone H3 acetylation at the BMP7 promoter after C4 (0.25 μM) treatment. Data represent mean ± SEM, $*P<0.05$, $**P<0.01$, $***P<0.001$. **(f)** ELISA analysis of BMP7. **(g)** Western blots of BMP7. DPSCs were cultured in mineralization medium or mineralization medium supplemented with C2 or C4 for 3 days before ELISA and for 7 days before western blotting of Psmad1/5/9 and BMP7. BMP, bone morphogenetic protein; ChIP, chromatin immunoprecipitation; ELISA, enzyme-linked immunosorbent assay; GAPDG, glyceraldehyde-3-phosphate dehydrogenase. Color images are available online.

BMP2, BMP4, and BMP7 promoters. A significant increase in histone acetylation at BMP7 promoter after C4 treatment (0.25 μM) was documented (Fig. 5e). We measured BMP7 expression in DPSCs after stimulation with C2 or C4. ELISAs of cell supernatants showed significantly increased BMP7 secretion (Fig. 5f) and western blotting showed increased protein expression (Fig. 5g; Supplementary Fig. S2c).

We also carried out BMP7 immunofluorescence staining in vivo. The staining showed that BMP7 expression in ABX mice was decreased (Fig. 6a). Double staining of BrdU and BMP7 showed a number of BrdU-expressing cells colocalizing with BMP7-positive cells, which confirmed that MSCs were the resource of BMP7. Compared with SPF mice, BMP7 and BrdU coexpression was decreased in ABX mice. After SCFAs supplementation, the coexpression in mice of SCFA group showed no difference compared with SPF mice (Fig. 6b). Taken together, these results suggested that SCFAs could promote histone acetylation and BMP7 transcription/synthesis of dental MSCs both in vivo and in vitro, which contributed to increased BMP signaling and dentinogenic differentiation.

Discussion

Microbiota are required for maintaining homeostasis and MSC function in multiple organs. In oral tissues, microbiota have been found to regulate gingival MSC regeneration. Antibiotic-altered oral microbiota and LPS levels would cause gingival MSC deficiency, which then leads to delayed wound healing in mice [7]. However, the effect of microbiota on incisor regeneration or dental MSCs has not been reported previously.

Our study indicated that normal microbiota are required for dental MSCs to maintain regeneration and differentiation. Microbiota took function by metabolizing SCFAs. In our study, we performed clipping to observe the incisor renewal rate under antibiotic treatment to explore the possible roles microbiota and their metabolite SCFAs may have on incisor regeneration. We found that antibiotic-induced depletion of microbiota caused reduction of the incisor renewal rate and SCFA levels. Supplementation of SCFAs in drinking water during antibiotic treatment could effectively rescue the incisor renewal rate, which indicated that SCFAs took part in maintaining incisor regeneration of mice.

Although epithelial stem cells were prominent in incisor turnover, we did not observe significant changes in their numbers. We hypothesized that MSCs may be more sensitive to microbiota alterations. Different to data from previous studies, MSC deficiency did not cause lower renewal rate directly. A reduced number of MSCs did not lead to a smaller population of TACs. Surprisingly, the number of TACs was similar among groups. Considering the number of TACs directed by the MSC-TAC transition and TAC-preodontoblast transition, we transferred our attention to the downstream TAC-preodontoblast/odontoblast transition and odontoblast differentiation.

It has been reported that SCFAs (especially C2 and C4) can regulate MSC differentiation. C4 can promote osteogenic differentiation of BMMSCs and adipose-derived stem cells in vivo or in vitro [31,32]. C4 can also induce differentiation of dental follicle cells in vitro [33]. We found that SCFA deficiency induced by antibiotic treatment led to delayed odontoblast differentiation process in ABX mice, whereas supplementation with SCFAs could normalize odontoblast differentiation effectively. Furthermore, stimulation with C4 and C2 can promote odontoblast differentiation of DPSCs in vitro. We concluded that SCFAs can promote dentinogenesis in vivo and odontoblast differentiation of dental MSCs in vitro.

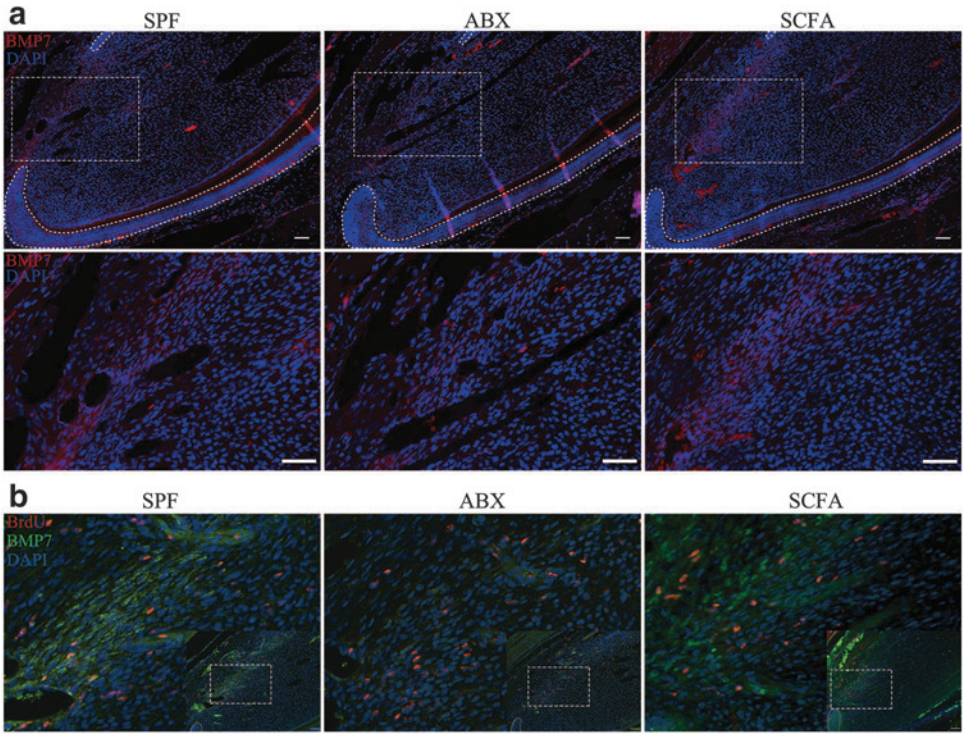

FIG. 6. SCFAs promote dental MSCs secreting BMP7. **(a)** Immunofluorescent staining of BMP7 (*red*) in incisors of mice in SPF, ABX, and SCFA groups. *Boxes* are magnified in the *second row*. **(b)** Double-immunofluorescent staining of BMP7 (*green*) and BrdU (*red*) in incisors of mice in SPF, ABX, and SCFA groups. Samples in **(a, b)** were collected 48 h after clipping. *Dotted lines* outlined the cervical loop dental epithelium. Cell nuclei were stained with DAPI (*blue*). $N = 3$–4, Scale bar: 50 μm. Color images are available online.

BMPs are a group of signaling molecules that belong to the transforming growth factor-β superfamily of proteins. BMP signaling is indispensable for tissue regeneration and can regulate the proliferation and osteogenic differentiation of stem cells [34,35]. In classic osteoclast differentiation, BMPs transduce their signaling activity by phosphorylating the transcription factors, Smads 1, 5, and/or 8, which, in turn, form a heterodimeric complex with Smad4 and regulate downstream targets in concert with coactivators [36–38]. In mouse incisors, activated BMP signaling maintains TACs-preodontoblasts/odontoblasts transition and odontoblast differentiation. Loss of BMP signaling leads to compromised odontoblast differentiation and incisor growth defects [30].

In our study, we found that activated BMP signaling was downgraded after antibiotic treatment. Thus, we concluded that SCFA deficiency caused delayed odontoblast differentiation through downgrading of BMP signaling. Moreover, according to Shi et al., BMP signaling in the preodontoblast/odontoblast region can provide feedback to MSCs in the mouse incisor to sustain the renewal ability and population of MSCs [30]. A reduced number of dental MSCs in ABX mice were observed in our study. Since we did not observe increased apoptosis in MSC zone (Supplementary Fig. S2b), and our in vitro colony assay also suggested the impaired self-renewal ability of MSCs, the diminished MSC population was likely due to the decreased feedback from BMP signaling in preodontoblast/odontoblast region (Fig. 3c).

Epigenetic modifications of the chromatin structures, including histone deacetylations mediated by HDACs, have an essential role in regulating stem cell pluripotency and progenitor reprogramming. BMMSCs are affected by HDAC inhibitors with regard to osteogenic differentiation in vitro and bone formation in vivo [28]. HDAC inhibitors have also shown to induce differentiation and accelerated mineralization of dental stem cells or pulp-derived cells in vitro [39–41]. SCFAs are effective inhibitors of HDACs. It has been proved that the regulatory effects of SCFAs on the differentiation of stem cells were due to their ability to inhibit HDACs.

Among all types of SCFAs, C4 is the most active HDAC inhibitor, whereas C2 has very low inhibitory activity [42]. Some studies have found that C2 is inactive in suppressing HDACs in some cells [17,43]. Other researchers have concluded that acetyl-coenzyme A (CoA) derived from acetate supplementation increases histone acetylation state by reducing HDAC activity/expression [44,45]. In brief, it is difficult for C2 to suppress HDAC activity directly, but C2 supplementation can cause HDAC inhibition in an acetyl-CoA-based way. In our study, an increase in histone acetylation of DPSCs stimulated with C2 or C4 was observed. We hypothesized that SCFAs may take function by inhibiting HDACs activity and increasing acetylation.

According to the study, BMP9-induced expression of osteogenic markers osteopontin and osteocalcin, as well as bone formation, are augmented significantly by HDAC inhibitors. [29]. Thus, we suggest that enhancement by SCFAs of DPSC differentiation may be related to increased transcription of BMP signaling molecules followed by HDAC activity inhibition. Accordingly, ChIP assays showed that SCFAs could promote BMP7 expression by suppressing HDAC activity. The increased expression of BMP7 after treatment with C2 or C4 verified our hypothesis. According to previous studies, BMP7 indeed can enhance DPSC differentiation toward an odontoblast-like phenotype in vitro and in vivo [46,47].

According to previous studies, BMP, FGF, and Wnt signaling pathways were related to odontoblast differentiation [22,35,48]. We examined their expression earlier and found increased BMP signaling activation after SCFA treatment. However, the expression of BMP2, BMP4, and BMP7 of DPSCs increased after SCFA stimulation in vitro (data not shown). The results of ChIP assay made us focus on BMP7. However, whether SCFAs promoted the expression of BMP2/4 and contributed to dentinogenic differentiation by HDAC-independent ways were not clear.

Microbiota and their metabolites, SCFAs, are crucial for incisor regeneration and differentiation of dental MSCs. SCFAs can promote TAC-preodontoblast/odontoblast transition and odontoblast differentiation in vivo and in vitro through increased BMP signaling through inhibition of HDACs. These results may assist our understanding of MSCs and provide some ideas for the improvements of MSC application. In addition, many previous studies suggested that the use of antibiotics is among the causative factors of molar incisor hypomineralization (MIH) [49–51]. However, the detailed role and mechanisms of antibiotics need to be further studied. We hope our study can make some help to MIH researches.

Acknowledgment

The authors thank the center laboratory of Peking University School and Hospital of Stomatology for providing the research facilities.

Author Disclosure Statement

No competing financial interests exist.

Funding Information

This work was supported by a grant from the National Natural Science Foundation of China (no. 81870816).

Supplementary Material

Supplementary Figure S1
Supplementary Figure S2

References

1. Xiao E, L He, Q Wu, J Li, Y He, L Zhao, S Chen, J An, Y Liu, C Chen and Y Zhang. (2017). Microbiota regulates bone marrow mesenchymal stem cell lineage differentiation and immunomodulation. Stem Cell Res Ther 8:213.
2. Lucas S, Y Omata, J Hofmann, M Bottcher, A Iljazovic, K Sarter, O Albrecht, O Schulz, B Krishnacoumar, et al. (2018). Short-chain fatty acids regulate systemic bone mass and protect from pathological bone loss. Nat Commun 9: 55.
3. Ohlsson C, G Nigro, IG Boneca, F Backhed, P Sansonetti and K Sjogren. (2017). Regulation of bone mass by the gut microbiota is dependent on NOD1 and NOD2 signaling. Cell Immunol 317:55–58.
4. Ohlsson C and K Sjogren. (2015). Effects of the gut microbiota on bone mass. Trends Endocrinol Metab 26:69–74.
5. Erny D, AL Hrabe de Angelis, D Jaitin, P Wieghofer, O Staszewski, E David, H Keren-Shaul, T Mahlakoiv, K

Jakobshagen, et al. (2015). Host microbiota constantly control maturation and function of microglia in the CNS. Nat Neurosci 18:965–977.
6. Yan J, JW Herzog, K Tsang, CA Brennan, MA Bower, WS Garrett, BR Sartor, AO Aliprantis and JF Charles. (2016). Gut microbiota induce IGF-1 and promote bone formation and growth. Proc Natl Acad Sci USA 113:E7554–E7563.
7. Su Y, C Chen, L Guo, J Du, X Li and Y Liu. (2018). Ecological balance of oral microbiota is required to maintain oral mesenchymal stem cell homeostasis. Stem Cells 36:551–561.
8. Rakoff-Nahoum S, J Paglino, F Eslami-Varzaneh, S Edberg and R Medzhitov. (2004). Recognition of commensal microflora by Toll-like receptors is required for intestinal homeostasis. Cell 118:229–241.
9. Medzhitov R. (2007). Recognition of microorganisms and activation of the immune response. Nature 449:819–826.
10. den Besten G, K van Eunen, AK Groen, K Venema, DJ Reijngoud and BM Bakker. (2013). The role of short-chain fatty acids in the interplay between diet, gut microbiota, and host energy metabolism. J Lipid Res 54:2325–2340.
11. Ríos-Covián D, P Ruas-Madiedo, A Margolles, M Gueimonde, CG de Los Reyes-Gavilán and N Salazar. (2016). Intestinal short chain fatty acids and their link with diet and human health. Front Microbiol 7:185.
12. Panasevich MR, WT Peppler, DB Oerther, DC Wright and RS Rector. (2017). Microbiome and NAFLD: potential influence of aerobic fitness and lifestyle modification. Physiol Genomics 49:385–399.
13. Schroeder BO and F Backhed. (2016). Signals from the gut microbiota to distant organs in physiology and disease. Nat Med 22:1079–1089.
14. Iván J, E Major, A Sipos, K Kovács, D Horváth, I Tamás, P Bay, V Dombrádi and B Lontay. (2017). The short-chain fatty acid propionate inhibits adipogenic differentiation of human chorion-derived mesenchymal stem cells through the free fatty acid receptor 2. Stem Cells Dev 26:1724–1733.
15. Park J-h, T Kotani, T Konno, J Setiawan, Y Kitamura, S Imada, Y Usui, N Hatano, M Shinohara, et al. (2016). Promotion of intestinal epithelial cell turnover by commensal bacteria: role of short-chain fatty acids. PLoS One 11:e0156334.
16. Wang Y, L Zhang, J Yu, S Huang, Z Wang, KA Chun, TL Lee, Y-T Chen, RL Gallo and C-M Huang. (2017). A co-drug of butyric acid derived from fermentation metabolites of the human skin microbiome stimulates adipogenic differentiation of adipose-derived stem cells: implications in tissue augmentation. J Invest Dermatol 137:46–56.
17. Waldecker M, T Kautenburger, H Daumann, C Busch and D Schrenk. (2008). Inhibition of histone-deacetylase activity by short-chain fatty acids and some polyphenol metabolites formed in the colon. J Nutr Biochem 19:587–593.
18. Ledesma-Martinez E, VM Mendoza-Nunez and E Santiago-Osorio. (2016). Mesenchymal stem cells derived from dental pulp: a review. Stem Cells Int 2016:4709572.
19. Zhao H, J Feng, K Seidel, S Shi, O Klein, P Sharpe and Y Chai. (2014). Secretion of Shh by a neurovascular bundle niche supports mesenchymal stem cell homeostasis in the adult mouse incisor. Cell Stem Cell 14:160–173.
20. Sharpe PT. (2016). Dental mesenchymal stem cells. Development 143:2273–2280.
21. An Z, M Sabalic, RF Bloomquist, TE Fowler, T Streelman and PT Sharpe. (2018). A quiescent cell population replenishes mesenchymal stem cells to drive accelerated growth in mouse incisors. Nat Commun 9:378.
22. Ishikawa Y, M Nakatomi, H Ida-Yonemochi and H Ohshima. (2017). Quiescent adult stem cells in murine teeth are regulated by Shh signaling. Cell Tissue Res 369:497–512.
23. Ishikawa Y, H Ida-Yonemochi, K Nakakura-Ohshima and H Ohshima. (2012). The relationship between cell proliferation and differentiation and mapping of putative dental pulp stem/progenitor cells during mouse molar development by chasing BrdU-labeling. Cell Tissue Res 348:95–107.
24. Nur Akmal MR, ZAI Zarina, MAW Rohaya, S Sahidan, ZA Zaidah and ZAS Hisham. (2014). Isolation and characterization of dental pulp stem cellsfrom murine incisors. J Biol Sci 14:327–331.
25. Grasa L, L Abecia, R Forcen, M Castro, JA de Jalon, E Latorre, AI Alcalde and MD Murillo. (2015). Antibiotic-induced depletion of murine microbiota induces mild inflammation and changes in Toll-like receptor patterns and intestinal motility. Microb Ecol 70:835–848.
26. Reikvam DH, A Erofeev, A Sandvik, V Grcic, FL Jahnsen, P Gaustad, KD McCoy, AJ Macpherson, LA Meza-Zepeda and FE Johansen. (2011). Depletion of murine intestinal microbiota: effects on gut mucosa and epithelial gene expression. PLoS One 6:e17996.
27. Seidel K, P Marangoni, C Tang, B Houshmand, W Du, RL Maas, S Murray, MC Oldham and OD Klein. (2017). Resolving stem and progenitor cells in the adult mouse incisor through gene co-expression analysis. Elife 6:e24712.
28. Xu S, K De Veirman, H Evans, GC Santini, I Vande Broek, X Leleu, A De Becker, B Van Camp, P Croucher, K Vanderkerken and I Van Riet. (2013). Effect of the HDAC inhibitor vorinostat on the osteogenic differentiation of mesenchymal stem cells *in vitro* and bone formation *in vivo*. Acta Pharmacol Sin 34:699–709.
29. Hu N, C Wang, X Liang, L Yin, X Luo, B Liu, H Zhang, W Shui, G Nan, et al. (2013). Inhibition of histone deacetylases potentiates BMP9-induced osteogenic signaling in mouse mesenchymal stem cells. Cell Physiol Biochem 32:486–498.
30. Shi C, Y Yuan, Y Guo, J Jing, T-V Ho, X Han, J Li, J Feng and Y Chai. (2019). BMP signaling in regulating mesenchymal stem cells in incisor homeostasis. J Dental Res 98:904–911.
31. Chen T-H, W-M Chen, K-H Hsu, C-D Kuo and S-C Hung. (2007). Sodium butyrate activates ERK to regulate differentiation of mesenchymal stem cells. Biochem Biophys Res Commun 355:913–918.
32. Hu X, Y Fu, X Zhang, L Dai, J Zhu, Z Bi, Y Ao and C Zhou. (2014). Histone deacetylase inhibitor sodium butyrate promotes the osteogenic differentiation of rat adipose-derived stem cells. Dev Growth Different 56:206–213.
33. Drees J, O Felthaus, M Gosau and C Morsczeck. (2014). Butyrate stimulates the early process of the osteogenic differentiation but inhibits the biomineralization in dental follicle cells (DFCs). Odontology 102:154–159.
34. Zhang J and L Li. (2005). BMP signaling and stem cell regulation. Dev Biol 284:1–11.
35. Luu HH, W-X Song, X Luo, D Manning, J Luo, Z-L Deng, KA Sharff, AG Montag, RC Haydon and T-C He. (2007). Distinct roles of bone morphogenetic proteins in osteogenic differentiation of mesenchymal stem cells. J Orthop Res 25:665–677.

36. Shi Y and J Massagué. (2003). Mechanisms of TGF-β signaling from cell membrane to the nucleus. Cell 113:685–700.
37. Jensen ED, L Pham, CJ Billington, Jr., K Espe, AE Carlson, JJ Westendorf, A Petryk, R Gopalakrishnan and K Mansky. (2010). Bone morphogenic protein 2 directly enhances differentiation of murine osteoclast precursors. J Cell Biochem 109:672–682.
38. Retting KN, B Song, BS Yoon and KM Lyons. (2009). BMP canonical Smad signaling through Smad1 and Smad5 is required for endochondral bone formation. Development 136:1093–1104.
39. Jin H, JY Park, H Choi and PH Choung. (2013). HDAC inhibitor trichostatin A promotes proliferation and odontoblast differentiation of human dental pulp stem cells. Tissue Eng Part A 19:613–624.
40. Duncan HF, AJ Smith, GJ Fleming and PR Cooper. (2012). Histone deacetylase inhibitors induced differentiation and accelerated mineralization of pulp-derived cells. J Endod 38:339–345.
41. Duncan HF, AJ Smith, GJ Fleming and PR Cooper. (2013). Histone deacetylase inhibitors epigenetically promote reparative events in primary dental pulp cells. Exp Cell Res 319:1534–1543.
42. Boffa LC, G Vidali, RS Mann and VG Allfrey. (1978). Suppression of histone deacetylation *in vivo* and *in vitro* by sodium butyrate. J Biol Chem 253:3364–3366.
43. Kiefer J, G Beyer-Sehlmeyer and BL Pool-Zobel. (2006). Mixtures of SCFA, composed according to physiologically available concentrations in the gut lumen, modulate histone acetylation in human HT29 colon cancer cells. Br J Nutr 96:803–810.
44. Soliman ML and TA Rosenberger. (2011). Acetate supplementation increases brain histone acetylation and inhibits histone deacetylase activity and expression. Mol Cell Biochem 352:173–180.
45. Soliman ML, MD Smith, HM Houdek and TA Rosenberger. (2012). Acetate supplementation modulates brain histone acetylation and decreases interleukin-1β expression in a rat model of neuroinflammation. J Neuroinflammation 9:51.
46. Yang X, G Han, X Pang and M Fan. (2012). Chitosan/collagen scaffold containing bone morphogenetic protein-7 DNA supports dental pulp stem cell differentiation *in vitro* and *in vivo*. J Biomed Mater Res Part A. DOI: 10.1002/jbm.a.34064.
47. Paiva K, L Silva, M Sogayar and L Labriola. (2014). Differential gene expression of matrix metalloproteinases (MMPs) and their tissue inhibitors (TIMPs) are modulated during osteogenic/odontogenic differentiation from human dental pulp stem cells (DPSCs) by BMP-7. Bone Abstracts 3:147. DOI: 10.1530/boneabs.3.PP147.
48. Scheller EL, J Chang and CY Wang. (2008). Wnt/β-catenin inhibits dental pulp stem cell differentiation. J Dent Res 87:126–130.
49. Laisi S, A Ess, C Sahlberg, P Arvio, PL Lukinmaa and S Alaluusua. (2009). Amoxicillin may cause molar incisor hypomineralization. J Dent Res 88:132–136.
50. Kuscu OO, N Sandalli, S Dikmen, O Ersoy, I Tatar, I Turkmen and E Caglar. (2013). Association of amoxicillin use and molar incisor hypomineralization in piglets: visual and mineral density evaluation. Arch Oral Biol 58:1422–1433.
51. Giuca MR, M Cappe, E Carli, L Lardani and M Pasini. (2018). Investigation of clinical characteristics and etiological factors in children with molar incisor hypomineralization. Int J Dent 2018:7584736.

Address correspondence to:
Yuming Zhao, DDS, MD
Department of Pediatric Dentistry
School and Hospital of Stomatology
Peking University
Beijing 100081
China

E-mail: yuming_zhao@hotmail.com

E. Xiao, PhD
Department of Oral and Maxillofacial Surgery
School and Hospital of Stomatology
Peking University
Beijing 100081
China

E-mail: xiaoe1986@vip.163.com

Received for publication March 22, 2020
Accepted after revision July 20, 2020
Prepublished on Liebert Instant Online July 21, 2020